CHEMISTRY
A EUROPEAN JOURNAL

COMMUNICATION

DOI: 10.1002/chem.201301481

Platinum(II) and Gold(III) Allenylidene Complexes: Phosphorescence, Self-Assembled Nanostructures and Cytotoxicity

Xin-Shan Xiao,[a] Wai-Lun Kwong,[a] Xiangguo Guan,[a] Chen Yang,[a] Wei Lu,*[b] and Chi-Ming Che*[a, c]

Luminescent metal–carbon complexes are well documented to have enormous impact to the development of materials science and photochemistry.[1] We and others have been working on the synthesis of new phosphorescent organometallic complexes containing acetylide[2] and N-heterocyclic carbene (NHC)[3] ligands and their applications in high-performance OLEDs, nonlinear optics, chemosensors, bioprobes and photocatalysts. Along this line of research, cumulenic metal complexes with long-lived excited-states could be a starting point of investigation on new classes of phosphorescent metal–carbon bonded complexes.

Cumulene is a reactive functional group but its stability can be enhanced upon coordination to a metal ion.[4] Metal complexes with an allenylidene (the C_3 homologue of cumulene) ligand continue to attract much attention since the isolation of first stable allenylidene complexes by Fischer and Berke in 1976.[5] The σ-donation from α-carbon (C_α) and π-interaction between metal ion and the linear allenylidene bridge strengthen the M−C_α bond, and hence render the metal ion an intriguing site for catalysis and the allenylidene ligand a conductive wire for charge transport.[6] Although a variety of [L_nM=C=C=C(R′)R″] complexes, in which M is metal ion of Cr, W, Mn, Ru, Os, Ir, Ag, Pd or Pt, have been prepared,[4,7] only two types of allenylidene complexes have been reported to display phosphorescence. Slageren and co-workers reported that [Cl(dppm)$_2$Ru=C=C=C(R′)R″] complexes are emissive in glassy solutions at 93 K.[8] Nazeeruddin and co-workers claimed [(ppy)$_2$(Ph_3P)Ir=C=C=C-(OMe)N(CH_2)$_4$]$^+$ to be the first allenylidene complex that emits in fluid solutions (with an emission quantum yield of 2.9% and a lifetime of 465 ns).[9] Herein, we describe two Pt^{II} and two Au^{III} allenylidene complexes (Scheme 1) supported by tridentate cyclometalated ligands having mixed N- and C-donor atoms, three of which show phosphorescence in solutions at room temperature. These metal–allenylidene complexes exhibit many intriguing functionalities including self-assembled nanostructures and biological activity. The present work features the first report on Au^{III} allenylidene complexes. Just recently, Hashmi and co-workers reported the X-ray crystal structure of the first Au^{I} allenylidene complex supported by a NHC ligand.[10]

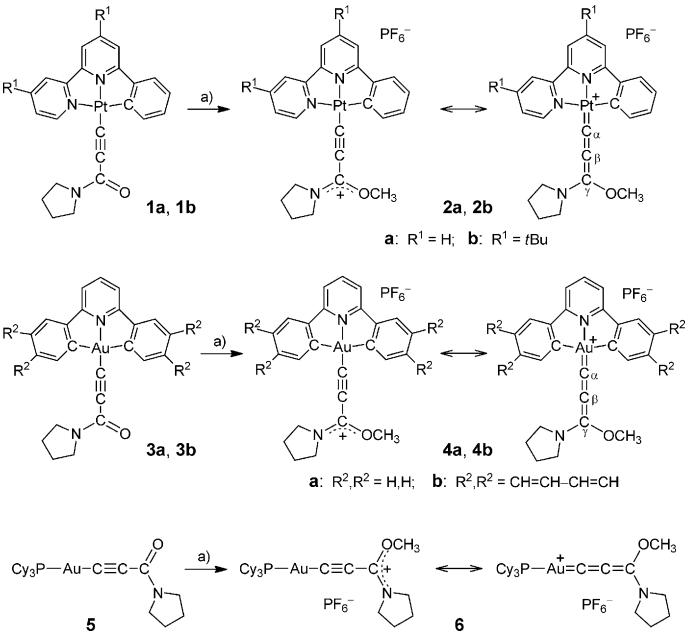

Scheme 1. Synthesis and mesomeric structures of the Pt^{II}, Au^{III} and Au^{I} allenylidene complexes. Reaction conditions: a) CH_3OTf, CH_2Cl_2, and then NH_4PF_6.

Our approach to phosphorescent Pt^{II} and Au^{III} allenylidene complexes is outlined in Scheme 1. First, the respective acetylide precursors (**1a**/**b** for Pt^{II} and **3a**/**b** for Au^{III}, Scheme 1) were prepared by a CuI-catalyzed reaction of [(C^N^N)PtCl] and [(C^N^C)AuCl] (both C^N^N and C^N^C represent π-conjugated cyclometalated/oligopyridyl ligands) with propargylic amine. Second, the heteroatom-

[a] X.-S. Xiao, W.-L. Kwong, Dr. X. Guan, C. Yang, Prof. Dr. C.-M. Che
State Key Laboratory of Synthetic Chemistry
Institute of Molecular Functional Materials
HKU-CAS Joint Laboratory on New Materials, and
Department of Chemistry, The University of Hong Kong
Pokfulam Road, Hong Kong (P.R. China)
E-mail: cmche@hku.hk

[b] Prof. Dr. W. Lu
Department of Chemistry
South University of Science and Technology of China
Shenzhen, Guangdong 518055 (P.R. China)
E-mail: luw@sustc.edu.cn

[c] Prof. Dr. C.-M. Che
HKU Shenzhen Institute of Research and Innovation
Shenzhen, Guangdong 518053 (P.R. China)

Supporting information for this article is available on the WWW under http://dx.doi.org/10.1002/chem.201301481.

conjugated allenylidene ligand was introduced to the cyclometalated metal complexes through methylation on the propiolamide moiety of the respective acetylide precursors (Scheme 1).[7c] A subsequent anion metathesis from OTf^- to PF_6^- precipitated the desired salts in 78–85% yields. The detailed procedures for the synthesis are provided in the Supporting Information. Complexes **2a/b** are dark colored solids whereas **4a/b** are yellowish in color. All of these complexes are stable towards air and moisture.

The ^1H NMR spectra of the Pt^{II} complexes **2a/b** and Au^{III} complexes **4a/b** in CD_3CN each exhibit two triplet peaks due to the two N-bound CH_2 groups at 3.70/4.00, 3.62/3.94, 3.73/4.02 and 3.65/3.99 ppm, respectively, revealing that the $C(sp^2)$–N bond in these complexes are refrained from free rotation in solutions. Compared with their corresponding acetylide precursors **1a/b** and **3a/b**, an additional singlet peak for the OCH_3 group at 4.39, 4.32, 4.40 and 4.42 ppm appears in the ^1H NMR spectra of **2a/b** and **4a/b**, respectively. The ^{13}C NMR signal for C_β of the allenylidene ligand in **2a/b** and **4a/b** can be clearly identified at 90.54, 91.77, 88.80 and 85.16 ppm, respectively, which are shifted upfield from that of **1a/b** and **3a/b** at 100.17, 100.08, 95.97, 92.90 ppm, respectively. The IR spectra of complexes **2a/b** and **4a/b** all show a sharp ν(C=C=C) band at 2078, 2075, 2148 and 2146 cm^{-1} respectively; these ν(C=C=C) values are shifted to lower-energy from the ν(C≡C) stretching bands of their acetylide precursors **1a/b** and **3a/b** at 2091, 2089, 2153 and 2149 cm^{-1}, respectively. These spectroscopic data lend support to the allenylidenic character in complexes **2a/b** and **4a/b**. However, the extents of both the upfield shift of the C_β signal and the lowering of the ν(C=C=C) are less significant when compared with that found for the related complexes $[Br(PPh_3)_2M{=}C{=}C{=}C(OMe)N(CH_2)_4]^+$ (M = Pd or Pt)[7c] but comparable with that observed for complex $[(ppy)_2(Ph_3P)Ir{=}C{=}C{=}C(OMe)N(CH_2)_4]^+$.[9] Thus, the acetylide mesomeric structures have to be considered in the description of their overall bonding interactions as depicted in Scheme 1.

The X-ray crystal structures of **2a** and **4a** have been determined.[11] Perspective views of their complex cations are shown in Figure 1 a and b, respectively; detailed crystal data are provided in the Supporting Information. Both the Pt atom in **2a** and Au atom in **4a** adopt a distorted square-planar geometry. The Pt1–C17 length of 1.925(8) Å in **2a** is shorter than the Pt–C_α(≡C_β) and Pt–C_α(NHC) lengths of 1.957(9)–1.98(1) Å and 1.982–2.016 Å, respectively, found in the related [(C^N^N)PtC≡CR][2b] and [(C^N^N)Pt-(NHC)]$^+$[3c] complexes. The Au1–C18 length of 1.956(6) Å in **4a** is only slightly shorter than the Au–C_α(≡C_β) and Au-C_α(NHC) length of 1.967–2.008 Å and 1.967–2.017 Å, respectively, found in the related [(C^N^C)AuC≡CR][2d] and [(C^N^C)Au(NHC)]$^+$[3a] complexes. The C17–C18 length of 1.22(1) Å in **2a** and C18–C19 length of 1.208(8) Å in **4a** are slightly longer than the $C_\alpha{\equiv}C_\beta$ bond generally observed for Pt^{II} (typically 1.18 Å)[2b] and Au^{III} (typically 1.19 Å)[2d] acetylide complexes. These bond lengths reveal allenylidenic character in complexes **2a** and **4a**. In the crystal structures

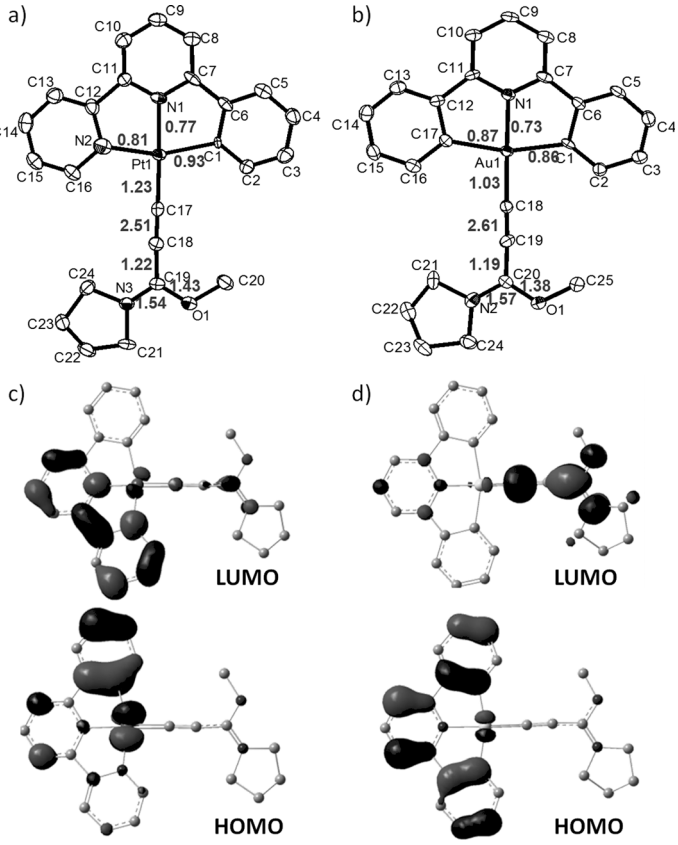

Figure 1. Perspective views of the cations of: a) Pt^{II} allenylidene complex **2a**, and b) Au^{III} allenylidene complex **4a**, determined with X-ray crystallography, with hydrogen atoms and counter-ions omitted for clarity. The Wiberg bond orders calculated based on the crystallographic parameters are shown as bold numbers. Frontier orbitals of: c) **2a**, and d) **4a**, calculated based on the crystallographic geometries.

of **2a** and **4a**, the complex cations are stacked in pairs in a head-to-tail fashion, with an interplanar π–π separation of around 3.4 Å. For **2a**, the intermetal distance of 3.29 Å is shorter than the sum of van der Waals radii of two Pt atoms (3.44 Å) and, together with the dark color of this complex in solid state, reveals remarkable intermolecular Pt···Pt interactions in the crystal structure.

The Wiberg bond orders in **2a** and **4a** are shown in Figure 1 as bold numbers. A comparison in bond orders between the structures of **2a** and **4a** shows that the allenylidenic character is more significant in **2a** (Pt–C_α 1.23, C_α–C_β 2.51 and C_β–C_γ 1.22) than that in **4a** (Au–C_α 1.03, C_α–C_β 2.61 and C_β–C_γ 1.19). This is consistent with the stronger π-back-donating capability of Pt^{II} than Au^{III}. The bond orders of C_γ–N and C_γ–O in **2a** (1.54 and 1.53) and **4a** (1.57 and 1.38) are larger than a single bond, indicating that the acetylide mesomeric structures (Scheme 1) weigh in the bonding structures of these complexes, in line with the NMR spectroscopy and IR characterizations.

The electrochemical redox potentials of **1a/b**, **2a/b**, **3a/b** and **4a/b** were measured using 0.1 M nBu_4NPF_6 as supporting electrolyte in acetonitrile (for Pt^{II} complexes) or DMF (for Au^{III} complexes) and reported versus the Fc^+/Fc

couple. The oxidation (irreversible anode peak)/reduction (quasi-reversible) of 0.66/−1.61 V for **2a** and 0.79/−1.71 V for **2b** are anodically shifted from those of **1a** (0.49/−1.73 V) and **1b** (0.46/−1.84 V); this is consistent with an increased π-back-bonding donation from Pt to the allenylidene moiety. The electrochemical reduction of the Au^{III} complexes **3a/b** and **4a/b** are irreversible, but a similar shifting trend in cathode peak potentials has also been observed from the Au–acetylide (−1.83 V for **3a** and −1.96 V for **3b**) to Au–allenylidene (−1.62 V for **4a** and −1.59 V for **4b**) complexes.

The electronic absorption and emission data of complexes **2a/b** and **4a/b** together with their acetylide precursors **1a/b**, and **3a/b** are listed in the Supporting Information and the representative spectra for **2a** and **4b** are shown in Figure 2.

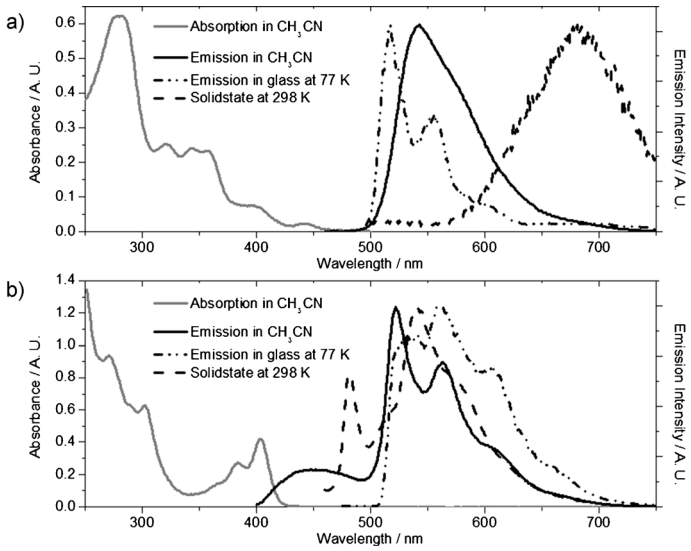

Figure 2. Absorption and normalized emission spectra of: a) **2a**, and b) **4b** in different matrixes.

To differentiate the absorption of allenylidene moiety from those of the cyclometalated ligand, a model complex, the heteroleptically coordinated allenylidene Au^{I} complex (**6**) was prepared from its acetylide precursor (**5**; Scheme 1). A CH_2Cl_2 solution of **6** shows a distinct lowest-energy absorption band at 278 nm (see the Supporting Information for a spectrum) and a structureless emission at $\lambda_{max}=416$ nm, revealing that ligand-centered transitions of the allenylidene moiety itself do not occur at spectral region beyond 300 nm. Solutions of complexes **2a** and **2b** in CH_2Cl_2 are yellow with a modest low-energy absorption band at $\lambda_{max}=400$ nm. When the concentration of **2a** in CH_2Cl_2 is increased beyond 2×10^{-5} M, an additional distinct absorption band emerges at $\lambda_{max}=440$ nm; this band is tentatively ascribed to a MMLCT transition derived from molecular aggregates through Pt···Pt interactions. The absence of MMLCT absorption band in the case of **2b** is attributed to the two bulky *tert*-butyl groups disfavoring intermolecular stacking interactions in solution. As for **4a** and **4b**, their absorption spectra display characteristic features as that of other Au^{III} complexes having the same cyclometalating ligands, which are mainly attributed to intraligand charge transfer (ILCT) transitions.[12] The frontier molecular orbitals (FMO) calculated based on crystallographic geometries of **2a** and **4a** are shown in Figure 1c and d, respectively. The electron density in HOMO and LUMO of **2a** are mainly localized on the Pt *d*-orbital/phenyl of C^N^N and bipyridyl of C^N^N, respectively, revealing a mixture of MLCT/ILCT transitions to account for the lowest-energy absorption of **2a**. The electron density in HOMO and LUMO of **4a** are mainly localized on the C^N^C and allenylidene ligand, respectively, revealing a LLCT transition to be responsible for the lowest-energy absorption of **4a**.

Upon excitation beyond 400 nm, Pt^{II} complexes **2a** and **2b** in diluted and degassed CH_2Cl_2 solutions show strong yellow-green emission with λ_{max} (quantum yield, lifetime) of 542 nm (34%, 3.9 μs) and 530 nm (63%, 4.5 μs), respectively. Based on the T1 optimized geometries, the TDDFT approach associated with the polarized continuum model (PCM) in CH_2Cl_2 was used to calculate the emission properties. To better describe the charge-transfer character of the electronic excitation of **2a** and **2b**, the density functional ωB97X-D,[13] which includes 100% long-range exact exchange, 22% of short-range exact exchange, the B97 correlation density functional,[14] and empirical dispersion corrections, was employed for the TDDFT calculations. The calculated triplet emissions of **2a** and **2b** in solutions are in the 520–525 nm region; this is in good agreement with the emission data from experiments. These emissions can be attributed to ^{3}MLCT/ILCT excited states with reference to previous works on cyclometalated Pt^{II} complexes.[15] Complex **2a** exhibits an emission maximum at 683 nm whereas the emission of **2b** is markedly red-shifted to the NIR region ($\lambda_{max}=$ 785 nm). On the other hand, the Au^{III} complex **4b** having extended C^N^C ligand gives dual emission bands in diluted, degassed CH_2Cl_2 solution upon excitation at 385 nm; the weak band at around 450 nm and the vibronically structured band at 525 nm (with a quantum yield of 3.3% and a lifetime of 111 μs) are ascribed to excited states having singlet and triplet ILCT origin, respectively.[12] Although **4a** is weakly emissive in solutions, it shows an intense bright-yellow emission at λ_{max} of 540 nm (with a lifetime of 5.8 μs) upon excitation at 350 nm in solid state at 298 K. The blue-shift emission of **4a** with respect to **2a** is due to the higher π* (LUMO) energy of allenylidene than that of bipyridyl moiety of C^N^N.

The combination of a planar cationic structure and intriguing phosphorescent properties renders these metal allenylidene complexes to potentially act as efficient switched-on probes for DNA molecules in aqueous solutions. Thus, an emission titration was performed with solutions of **2a** and **2b** (2 μM) in Tris-buffered saline/DMSO (3 mL, 99:1 v/v) by aliquots of a calf thymus DNA (ctDNA) stock solution (37 mM). As depicted in Figure 3a, upon increasing the ctDNA concentration from 0 to 3.6×10^{-4} M in intervals of

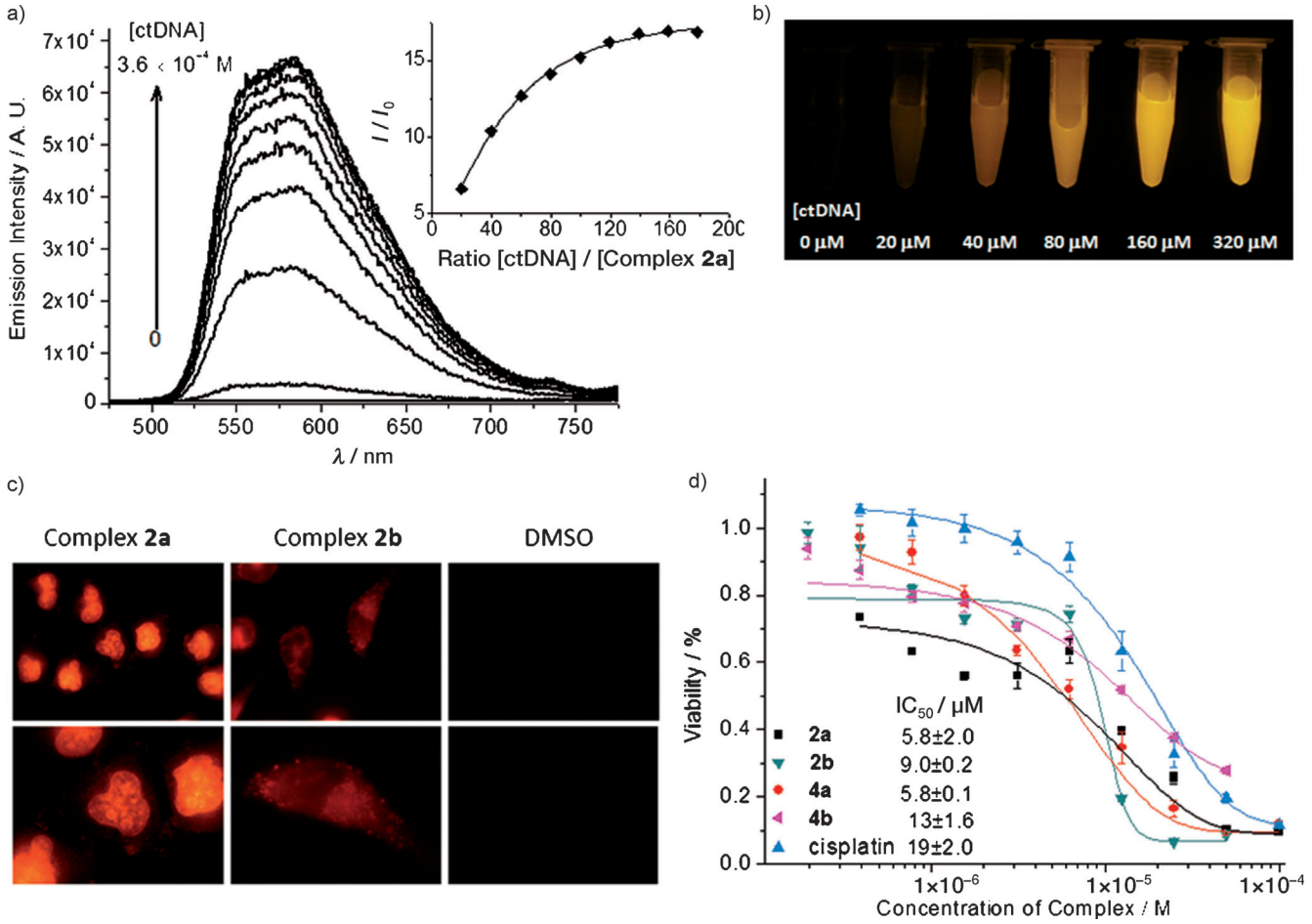

Figure 3. a) Emission traces of **2a** (2 μM) with increasing concentration of calf thymus DNA (ctDNA) in Tris-HCl (5 mM) buffer and NaCl (50 mM) at pH 7.2. Inset: response curve of I/I_o against [ctDNA]/[**2a**]. b) Image of **2a** (20 μM in buffer) in the presence of ctDNA on a transilluminator. Enhanced emission of **2a** was observed with increasing ctDNA concentration. c) Cellular imaging of **2a** and **2b** in viable HeLa cells, observed under fluorescence microscope with 100× oil immersed objective (excitation: 450 nm). Lower panel shows the enlarged images revealing the subcellular localization of **2a** and **2b**. d) Cytotoxicity profiles of complex **2a**, **2b**, **4a** and **4b** towards HeLa cells as determined by MTT assay; cisplatin was used as a control.

4.0×10^{-5} M, an emission band with λ_{max} at approximately 580 nm for **2a**/565 nm for **2b** developed and finally reached 17-fold for **2a**/fivefold for **2b** enhancement in intensity. The emission enhancement could be visualized with the naked eye (Figure 3b). We thus further investigated the applications of these complexes in cell imaging. HeLa cells (15×10^4) were treated with **2a** or **2b** (20 μM) for 2 h at 37 °C. Observation under a fluorescence microscope equipped with 450 nm excitation filter (Figure 3c) revealed living cell morphologies with **2a** predominately localized in the nucleus whereas **2b** mainly accumulated in the cytosolic region. The bulky *tert*-butyl groups in **2b** may impede the deep intercalation of **2b** into DNA and hence entry into the nucleus. The in vitro cytotoxicity of complexes **2a**, **2b**, **4a** and **4b** towards HeLa cells were evaluated by using the MTT assays. As depicted in Figure 3d, complexes **2a** and **4a** with IC_{50} (48 h incubation) values of 5.8 and 9.0 μM, respectively, are more cytotoxic than cisplatin ($IC_{50}=19$ μM in the control experiment).

The metal···metal and π–π interactions of these allenylidene complexes could act as the driving force for self-assembly of nanostructures.[16] Figure 4 depicts the morphologies of the nanostructures obtained with **2a** in solvent mixtures of CH_3CN/H_2O at various volumetric ratios. Nanorods (typically 200 nm wide and several micrometers long) and nanorings (typically 400 nm in outer diameter and 50 nm in inner diameter) were observed by electron microscopy as dominant morphologies in the 95:5 and 80:20 volumetric ratios of CH_3CN/H_2O, respectively. Some intermediate morphologies, such as bent nanorods and semicircles, were also detected when the volumetric ratio of CH_3CN/H_2O was 90:10 or 85:15 (see the Supporting Information for micrographs). Thus, increasing the water fraction in the solvent mixture facilitated the rod-to-ring transformation process. Interestingly, all the rods and rings were crystalline in nature, showing a typical *d*-spacing of 3.4 Å along the rod longitude and the ring periphery in their SAED patterns. This is evidence that metallophilic and ligand π–π interactions play a key role in the self-assembled formation of the intriguing nanostructures.

The nanostructures formed by complexes **2b** and **4b** were also studied for comparison (see the Supporting Information

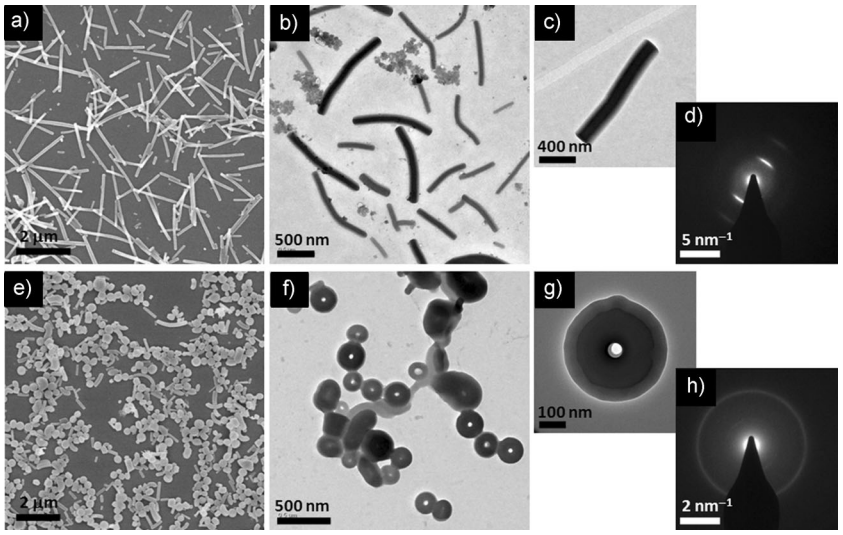

Figure 4. Micrographs (a and e, SEM; b, c, f, and g, TEM; d and h, SAED) of nanostructures self-assembled from **2a** in mixtures of CH_3CN/H_2O (95:5 (v/v) for a–d and 80:20 (v/v) for e–h). The TEM images have been rotated 92° so that the diffraction pattern coincides in orientation with the image.

for micrographs). All samples were obtained by air-drying diluted acetonitrile solutions of the metal allenylidene complexes on a silicon wafer or copper grid. TEM micrographs of **2b** showed uniformly spread nanospheres with average diameter of 200 nm. The absence of nanofibers with **2b** is attributed to the *tert*-butyl groups, which disfavor extensive one-dimensional packing of the Pt^{II} cations. In addition, the SEM micrographs of **4b** demonstrated an entangled fibrillar network, providing evidence for potential self-assembly behavior of the Au^{III} allenylidene complexes in solutions.

In summary, new Pt^{II} and Au^{III} allenylidene complexes have been prepared and found to display promising properties, such as prominent phosphorescence, self-assembling capability (into nanostructures), and cellular imaging and efficient cytotoxic activities. The applications of metal allenylidene complexes could be as rich as that of metal acetylide complexes, but allenylidene ligands would provide a new dimension for modification of the electronic structures and properties of the metal complexes. We thus envisage that luminescent metal–allenylidene complexes with long-lived excited states provide an entry to new classes of functional molecular materials and to supramolecular science with a bright future.

Acknowledgements

This work was supported by National Key Basic Research Program of China (973 Program 2013CB834802 and 2013CB834803) and the Hong Kong Research Grants Council (HKU 7011/07P and 7008/09P).

Keywords: allenylidene · gold · luminescence · platinum · self-assembly

[1] a) A. J. Lees, *Chem. Rev.* **1987**, *87*, 711–743; b) M. A. Baldo, M. E. Thompson, S. R. Forrest, *Nature* **2000**, *403*, 750–753; c) V. W.-W. Yam, K. K.-W. Lo, K. M.-C. Wong, *J. Organomet. Chem.* **1999**, *578*, 3–30; d) S. W. Lai, C. M. Che, *Top. Curr. Chem.* **2004**, *241*, 27–63; e) L. Flamigni, A. Barbieri, C. Sabatini, B. Ventura, F. Barigelletti, *Top. Curr. Chem.* **2007**, *281*, 143–203; f) K. M.-C. Wong, V. W.-W. Yam, *Acc. Chem. Res.* **2011**, *44*, 424–434; g) J. Kalinowski, V. Fattori, M. Cocchi, J. A. G. Williams, *Coord. Chem. Rev.* **2011**, *255*, 2401–2425; h) P.-T. Chou, Y. Chi, M.-W. Chung, C.-C. Lin, *Coord. Chem. Rev.* **2011**, *255*, 2653–2665; i) K. K.-W. Lo, A. W.-T. Choi, W. H.-T. Law, *Dalton Trans.* **2012**, *41*, 6021–6047; j) Y. You, W. Nam, *Chem. Soc. Rev.* **2012**, *41*, 7061–7084.

[2] a) R. H. Friend, R. W. Gymer, A. B. Holmes, J. H. Burroughes, R. N. Marks, C. Taliani, D. D. C. Bradley, D. A. Dos Santos, J. L. Bredas, M. Logdlund, W. R. Salaneck, *Nature* **1999**, *397*, 121–128; b) W. Lu, B.-X. Mi, M. C.-W. Chan, Z. Hui, N. Zhu, S.-T. Lee, C.-M. Che, *Chem. Commun.* **2002**, 206–207; c) V. W.-W. Yam, K. M.-C. Wong, N. Zhu, *J. Am. Chem. Soc.* **2002**, *124*, 6506–6507; d) K. M.-C. Wong, L.-L. Hung, W. H. Lam, N. Zhu, V. W.-W. Yam, *J. Am. Chem. Soc.* **2007**, *129*, 4350–4365; e) F. Camerel, R. Ziessel, B. Donnio, C. Bourgogne, D. Guillon, M. Schmutz, C. Iacovita, J. P. Bucher, *Angew. Chem.* **2007**, *119*, 2713–2716; *Angew. Chem. Int. Ed.* **2007**, *46*, 2659–2662; f) Y. Chen, K. Li, W. Lu, S. S. Y. Chui, C. W. Ma, C. M. Che, *Angew. Chem.* **2009**, *121*, 10093–10097; *Angew. Chem. Int. Ed.* **2009**, *48*, 9909–9913; g) W. Lu, W.-M. Kwok, C. Ma, C. T.-L. Chan, M.-X. Zhu, C.-M. Che, *J. Am. Chem. Soc.* **2011**, *133*, 14120–14135; h) W. Lu, K. T. Chan, S.-X. Wu, Y. Chen, C.-M. Che, *Chem. Sci.* **2012**, *3*, 752–755.

[3] a) V. K.-M. Au, K. M.-C. Wong, N. Zhu, V. W.-W. Yam, *J. Am. Chem. Soc.* **2009**, *131*, 9076–9085; b) J. J. Yan, A. L.-F. Chow, C.-H. Leung, R. W.-Y. Sun, D.-L. Ma, C.-M. Che, *Chem. Commun.* **2010**, *46*, 3893–3895; c) R. W.-Y. Sun, A. L.-F. Chow, X.-H. Li, J. J. Yan, S. S.-Y. Chui, C.-M. Che, *Chem. Sci.* **2011**, *2*, 728–736; d) K. Li, Y. Chen, W. Lu, N. Zhu, C.-M. Che, *Chem. Eur. J.* **2011**, *17*, 4109–4112; e) L. Mercs, M. Albrecht, *Chem. Soc. Rev.* **2010**, *39*, 1903–1912.

[4] a) M. I. Bruce, *Chem. Rev.* **1991**, *91*, 197–257; b) M. I. Bruce, *Chem. Rev.* **1998**, *98*, 2797–2858; c) V. Cadierno, S. E. García-Garrido, *Top. Organomet. Chem.* **2010**, *30*, 219–252.

[5] a) E. O. Fischer, H. J. Kalder, A. Frank, F. H. Kçhler, G. Huttner, *Angew. Chem.* **1976**, *88*, 683–684; *Angew. Chem. Int. Ed. Engl.* **1976**, *15*, 623–624; b) H. Berke, *Angew. Chem.* **1976**, *88*, 684; *Angew. Chem. Int. Ed. Engl.* **1976**, *15*, 624.

[6] a) P. F. H. Schwab, M. D. Levin, J. Michl, *Chem. Rev.* **1999**, *99*, 1863–1934; < lit b > C.-Y. Wong, G. S. M. Tong, C.-M. Che, N. Zhu, *Angew. Chem.* **2006**, *118*, 2760–2764; *Angew. Chem. Int. Ed.* **2006**, *45*, 2694–2698; c) R. F. Winter, S. ZáliŠ, *Coord. Chem. Rev.* **2004**, *248*, 1565–1583; d) C. Coletti, A. Marrone, N. Re, *Acc. Chem. Res.* **2012**, *45*, 139–149.

[7] Recent examples: a) F. Kessler, N. Szesni, K. Põhako, B. Weibert, H. Fischer, *Organometallics* **2009**, *28*, 348–354; b) M. Asay, B. Donnadieu, W. W. Schoeller, G. Bertrand, *Angew. Chem.* **2009**, *121*, 4890–4893; *Angew. Chem. Int. Ed.* **2009**, *48*, 4796–4799; c) F. Kessler, B. Weibert, H. Fischer, *Organometallics* **2010**, *29*, 5154–5161.

[8] J. van Slageren, R. F. Winter, A. Klein, S. Hartmann, *J. Organomet. Chem.* **2003**, *670*, 137–143.
[9] F. Kessler, B. F. E. Curchod, I. Tavernelli, U. Rothlisberger, R. Scopelliti, D. Di Censo, M. Grätzel, M. K. Nazeeruddin, E. Baranoff, *Angew. Chem.* **2012**, *124*, 8154–8157; *Angew. Chem. Int. Ed.* **2012**, *51*, 8030–8033.
[10] M. M. Hansmann, F. Rominger, A. S. K. Hashmi, *Chem. Sci.* **2013**, *4*, 1552–1559.
[11] CCDC-924251 (**2a**) and CCDC-924252 (**4a**) contain the supplementary crystallographic data for this paper. These data can be obtained free of charge from The Cambridge Crystallographic Data Centre via www.ccdc.cam.ac.uk/data_request/cif.
[12] W.-P. To, G. S.-M. Tong, W. Lu, C. Ma, J. Liu, A. L.-F. Chow, C.-M. Che, *Angew. Chem.* **2012**, *124*, 2708–2711; *Angew. Chem. Int. Ed.* **2012**, *51*, 2654–2657.
[13] J. D. Chai, M. Head-Gordon, *Phys. Chem. Chem. Phys.* **2008**, *10*, 6615–6620.
[14] A. D. Becke, *J. Chem. Phys.* **1997**, *107*, 8554–8560.
[15] W. Lu, M. C.-W. Chan, N. Zhu, C.-M. Che, C. Li, Z. Hui, *J. Am. Chem. Soc.* **2004**, *126*, 7639–7651.
[16] W. Lu, S. S.-Y. Chui, K.-M. Ng, C.-M. Che, *Angew. Chem.* **2008**, *120*, 4644–4648; *Angew. Chem. Int. Ed.* **2008**, *47*, 4568–4572.

Received: April 18, 2013
Published online: June 18, 2013

